[PS]Contrasting Abiotic and Biotic Processes in the Upper Barra Velha Formation at Iracema Field (Pre-Salt, Santos Basin)

Laís de Oliveira Ferreira[1], Michele Arena[1], Jane Nobre-Lopes[1], Josiane Plantz[1,2], Bruno Marques[1], and Leonardo Borghi[1]

Search and Discovery Article #51709 (2025)**
Posted November 7, 2025

*Adapted from extended abstract based on oral presentation given at AAPG International Conference and Exhibition (ICE) Rio de Janeiro, 30 September - 3 October, 2025.
 DOI:10.1306/51709Ferreira2025

[1]Geology Department, Federal University of Rio de Janeiro, Brazil
[2]Federal University of Uberlândia, Brazil

Abstract

The upper Aptian Barra Velha Formation (uBVF) has traditionally been interpreted as composed mainly of abiotic orthochemical deposits (travertines), reworked deposits, and calcilutites exhibiting microbial influence only at the top of the unit, particularly in the Lula Fingers. However, several abiotic and biotic processes interact in nature to impact the formation of travertines and microbialites. To better understand such interaction, and its impact on lithology classification, facies definition and depositional setting interpretations, we established meticulous micro- and macroscopic petrographic descriptions focusing on the identification of particular sedimentological features (textures, structures and fabric) of biotic and abiotic origins. Descriptions were made on 146 meters of cores and 60 thin sections, with alizarin-S staining, fluorescence and cathodoluminescence techniques, and SEM-EDS analysis from one well drilled through the uBVF at Iracema Field. Five lithotypes (calcilutites, spherulestones and hybrid forms, shrubstones, crustones and crystallines) and thirteen facies have been identified, six of them considered as bacterial-mediated in origin: 1.peloidal calcilutite, 2.wrinkly calcilutite, 3.muddy spherulestone, 4.microbial dolostone, 5. phytohermal crustone and 6. silicified microbial shrubstone; three facies are considered as inorganic precipitated with bacterial influence: 7. raft microcrystalline crustone, 8. laminated crustone, and 9. chert; five facies are considered as abiotic precipitated: 10. shrubby spherulestone, 11. hybrid spherulestone, 12. arborescent-arbustiform shrubstone and 13.dendriform shrubstone. Bacterial-mediated facies are more expressive but not restricted in the upper part of the core (44 m), and exhibit clotted texture, fenestral pores, tepees, microbial domes, and wrinkled laminae. These facies are interpreted as developed under shallow sub-aqueous environments presenting high rates of evaporation, biomineralization, and microbial trapping and binding. Inorganic precipitated with bacterial influence and abiotic facies occur in the lower and middle parts of the core (102 m), interbedded with clastic limestones (reworked facies not addressed in this study), and encompass features like crusts of calcite cement, shrub and raft crystals, clotted texture and possibly coated bubbles. These facies are interpreted as developed under very shallow waters eventually exposed to subaerial conditions as suggested by karstification features and early silicification; later, hydrothermal events seem to affect the interval. Our findings provide that organic remnants and microbial activity are not restricted to the Lula Fingers. Cathodoluminesce imaging effectively revealed multiple generations of late-stage calcite cements with dark brown to bright red concentric zoning; however, as this technique is not suited for identifying organic matter, it did not highlight remnants. In contrast, fluorescence microscopy proved to be the most effective

method, clearly identifying primary features such as filaments, biofilms, and microbial mats. Furthermore, fluorescence highlighted diagenetic characteristics such as engulfed and ghost minerals, organic nuclei, and porosity relationships, even in intensely dolomitized or recrystallized limestones. SEM-EDS analyses demonstrated that the organic tissues were replaced by extremely early silica, a common mechanism for preserving such remnants. The high thermal maturation of the Iracema Area is likely a key factor affecting the luminescence response of any remaining organic material.

Contrasting Abiotic and Biotic Processes in the Upper Barra Velha Formation at Iracema Field (Pre-salt, Santos Basin)

Laís de Oliveira Ferreira[1] *, Michele C. Arena[1] , Jane Nobre-Lopes[1] , Bruno M. Jesus[1] , Josiane Plantz[2] and Leonardo Borghi[1].

[1]*Laboratório de Geologia Sedimentar – LAGESED. Department of Geology, Federal University of Rio de Janeiro, CCMN, Cidade Universitária, Rio de Janeiro,*

[2]Federal University of Uberlândia, Uberlândia, Minas Gerais, Brazil *21941-916,*

** lais@geologia.ufrj.br*

Introduction

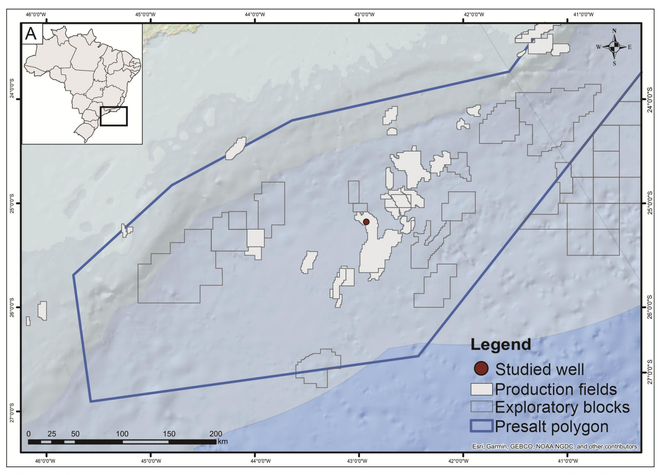

Figure 1: Location map of the studied well-core (red circle) in the Iracema Area of Tupi Field, Santos Basin.

The Aptian Mg-rich lacustrine carbonates of the upper Barra Velha Formation have recently been reinterpreted as abiotic chemical deposits (Wright and Barnet, 2015; Farias et al., 2019; Pietzsch et al., 2018; Basso et al., 2021) or as travertine facies (Falcão, 2015; Figueiredo et al., 2025), with microbial activity influencing carbonate deposition only at the top of the unit, particularly in the Lula Fingers ("Tupi/Lula Marker") (Carvalho and Fernandes, 2021; Rebelo et al., 2022; Plantz et al., 2024). These deposits are dominated by orthochemical constituents such as calcite fascicular shrubs, spherulites, siliciclastic and carbonate mud, and calcareous intraclasts. However, the formation of travertines and microbialites reflects the interplay between abiotic and biotic processes. Understanding this interaction is crucial, as it directly impacts lithological classification, facies definition, and interpretations of depositional settings.

In the studied core (Figure 1), abiotic carbonate-precipitated fabrics occur on decimeter- to millimeter-scales, whereas microbial mats are preserved at centimeter- to millimeter-scales. The preservation of microbial features in the studied area—such as microbial mats, filaments, encrusted biota (*sensu* Della Porta, 2015), and peloids—is highly significant, as it provides insights into the complex interplay between physico-chemical processes and microbial mats governing carbonate precipitation in the Iracema Area of Tupi Field.

Objective

- Investigate and compare the biotic and abiotic processes that influenced the upper Barra Velha Formation within the in-situ lithologies;
- Evaluate how analytical techniques such as cathodoluminescence, blue fluorescence, and scanning electron microscopy contribute to the identification of textures, structures, and biotic interactions across 146 meters of core comprising 60 thin sections using the classification scheme of Borghi et al., 2022.

Data and Method

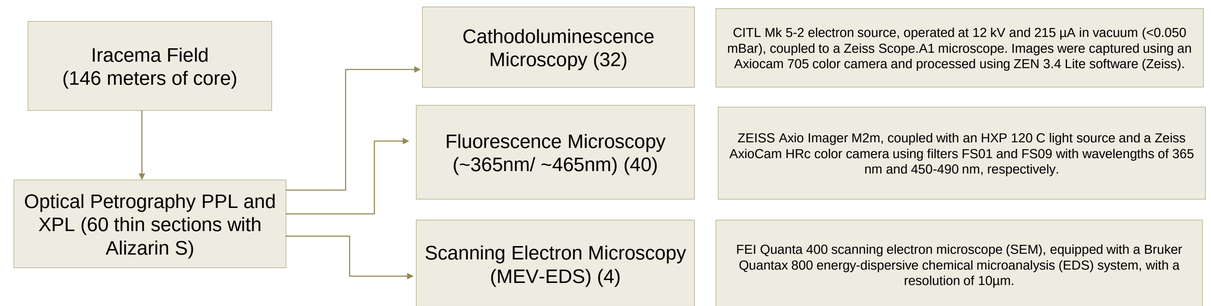

All analyses were carried out using equipment from the Sedimentary Geology Laboratory (Lagesed).

Results

CODE	LITHOFACIES	MAIN CONSTITUENTS	PROCESSES
CLU	Peloidal calcilutites (Strong recristalized)	Peloids, micropeloids, mud (micrite and clay minerals), detrital grains (quartz,mica, feldspar), spherulites and ostracod;	Microbially induced carbonate precipitation with sulfate-reducing bacteria
	Wrinkly calcilutites (Strong recristalized)	Microcrystalline calcite and dolomite, peloids, biofilms spherulites, detrital grains (quartz,mica, feldspar) and ostracod;	Microbially induced carbonate precipitation with sulfate-reducing bacteria
SPH	Muddy spherulestone	Spherulites, mud (micrite and clay minerals), peloids, detrital grains and ostracod;	1. Biologically influenced precipitated spherulites in organic rich muddy sediment; 2. Evaporation of lake waters, which led to the formation of authigenic mg-clays as clay gels and the nucleation and displacive growth of spherulites within this muddy material.
	Shrubby spherulestone	(Hybrid) spherulites, shrubs, mud (micrite and clay minerals) and calcispheres;	Lowering of the water table with intermittent mud precipitation; strong interactiong with lake bottom water or microbial mats
	Hybrid Spherulestone	(Hybrid) spherulites, shrubs, mud (micrite and clay minerals) and cacispheres;	Lowering of the water table with intermittent mud precipitation; strong interactiong with lake bottom water or microbial mats;
SHB	Arborescent shrubstone;	Arborescent and arbustiform shrubs, spherulites and calcispheres;	Abiotic precipitates formed by degassing in shallow water with moderate to intense, turbulent and hypersaturated in calcium carbonate flow. But may be mediated by the action of bacteria, and formation of biofilms;
	Silicified microbial shrubstone	Columnar shrubs, microbial mats, and calcispheres;	Biologically influenced precipitated shrubs linked to the decomposition of algal organic matter in an alkaline lacustrine environment.
	Dendriform shrubstone	Dendriform shrubs, peloids, ostracods and calcispheres;	Abiotic precipitates formed by degassing in shallow water with moderate to intense, turbulent and hypersaturated in calcium carbonate flow. But the action of bacteria, and formation of biofilms may played direct or indirect roles in lamination.
CRS	Phytohermal crustone	Encrusted micro-or macrophytes, (micro) peloids, calcispheres, and coated gas bubbles;	Biogenic calcification of stems from supersaturated water; supersaturation likely due to the photosynthetic effect in stagnant water
	Raft microcrystalline crustone	Rafts, (micro) peloids, micrite crusts, microbial mats, and coated grains;	Form on the water surface due to evaporation and temperature loss; May be mediated by bacteria;
	Laminated crustone	Shrubs, micrite, peloids;	Possibly micrite laminae correspond to an incrustations of algae (and/or other bacteria); associated to microbial biofilms
CRY	Dolostone	Rhombohedral dolomite, calcispheres;	Biogenically induced dolostone in a hypersaline, calm, and restricted setting with terrigenous inflow; linked to decomposition of algal organic matter;
	Chert	Chalcedony spherulites, microcrystalline quartz and macrocrystalline quartz	Biogenically induced chert linked to the decomposition of algal organic matter in an alkaline lacustrine environment.

Table 1: Lithofacies, main constituents, and processes involving the in-situ lithotypes Calcilutites (CLU), Spherulestones and hybrid forms (SPH), Shrubstones (SHB), Crustones (CRS), and Crystalline textures (CRY) observed in the studied core.

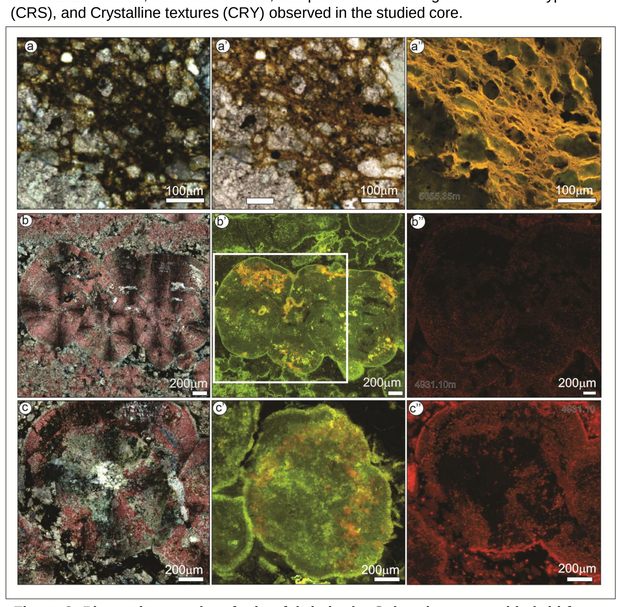

Figure 2: Photomicrographs of microfabric in the Spherulestone and hybrid forms lithotypes. (a, a', a") Preserved organic matter (lamalginite) shown in cross-polarized light (XPL) (a), plane-polarized light (PPL) (a'), and exhibiting high yellow fluorescence under UV light (a"). (b, b', b") Coalesced hybrid spherulites in XPL (b). Under UV light (b'), they show a bright orange fluorescence, indicative of contorted organic remnants or ferromanganese oxide coatings developed on the walls of the organic remnants. Cathodoluminescence (CL) (b") reveals a dull luminescence colour. (c, c', c") A spherulite intensely replaced by silica and celestine in XPL (c). UV light (c') shows incorporated organic material from during the replacement process. Cathodoluminescence (CL) (c") shows a dull luminescence pattern from the organic remnants and bright red luminescence from dolomite fringes.

Figure 3: Photomicrographs of microfabric in the Spheulestone and hybrid forms lithotypes. (a) Spherulites with rhomboedral dolomite and barite pore-filling in XPL. (a') non-fluorescence of spherulites under UV light, (a") CL image showing bright orange colors; (b) hybrid spherulites with silica and dolomite pore filling in XPL, (b') green dolomite fluorescence under UV light (b") bright dolomite fluorescence under UV light.

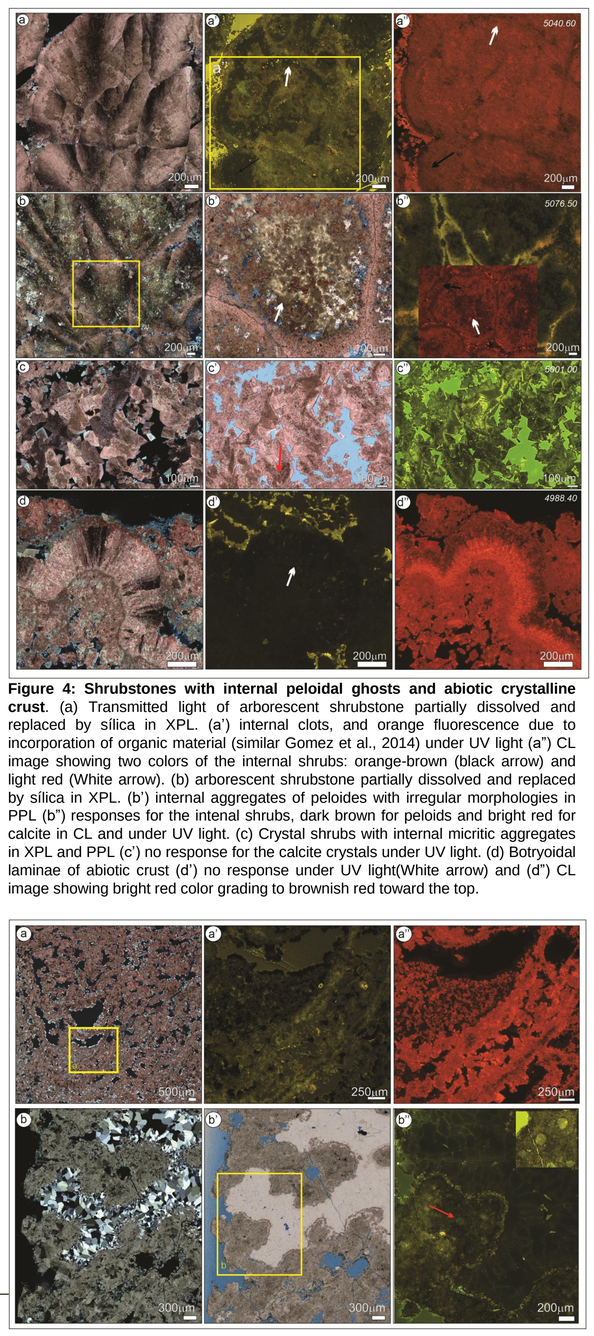

Figure 4: Shrubstones with internal peloidal ghosts and abiotic crystalline crust. (a) Transmitted light of arborescent shrubstone partially dissolved and replaced by sílica in XPL. (a') internal clots, and orange fluorescence due to incorporation of organic material (similar Gomez et al., 2014) under UV light (a") CL image showing two colors of the internal shrubs: orange-brown (black arrow) and light red (White arrow). (b) arborescent shrubstone partially dissolved and replaced by sílica in XPL. (b') internal aggregates of peloides with irregular morphologies in PPL (b") responses for the intenal shrubs, dark brown for peloids and bright red for calcite in CL and under UV light. (c) Crystal shrubs with internal micritic aggregates in XPL and PPL (c') no response for the calcite crystals under UV light. (d) Botryoidal laminae of abiotic crust (d') no response under UV light(White arrow) and (d") CL image showing bright red color grading to brownish red toward the top.

Figure 5 : Crustones as a product of microbially induced precipitation. (a) Peloidal-to-micropeloidal crustone with microbial contorted sheets and sílica coating the peloids and the sheets, XPL. (a') Light green fluorescence UV light. (a") CL images showing alternation in bright red and black colors. (b) Phytohermal crustone in XPL with sílica pore filling and (b') PPL, (b") Internal spheres (red arrow) with 100µm sized and light green fluorescence under UV light.

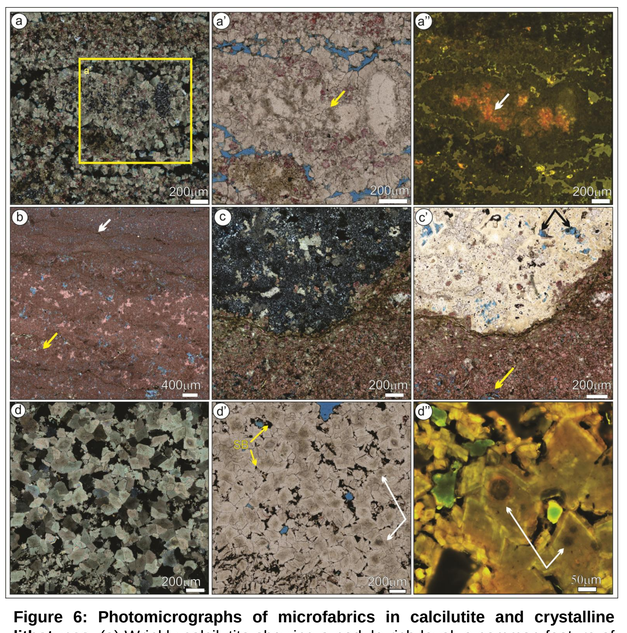

Figure 6: Photomicrographs of microfabrics in calcilutite and crystalline lithotypes. (a) Wrinkly calcilutite showing a nodule-rich level, a common feature of this facies, intensely replaced by microcrystalline quartz in XPL. In PPL (a'), a micrite rim is visible around the edges of nodules (yellow arrow) and numerous fluid inclusions. (a") Orange fluorescence (white arrow) response of an agglomerate of possible organic remnants under UV light. (b) Peloidal calcilutite/laminite showing peloids, ghosts of peloids (yellow arrow), microcrystalline calcite, pore-filling macrocrystalline calcite, and possible biofilms (white arrow). (c) and (c') Fenestral (black arrow) and intercrystalline porosities, biofilms, and ostracod bioclasts (yellow arrow) in XPL and PPL. (d) Dolostone with dirty center inside the crystals in XPL. (d') Dolostone showing intercrystalline porosity, irregular cloudy clots inside the crystals and solid bitumen (SB). (d") the same sample under UV light, possibly showing engulfed spheres of microfossils (white arrow).

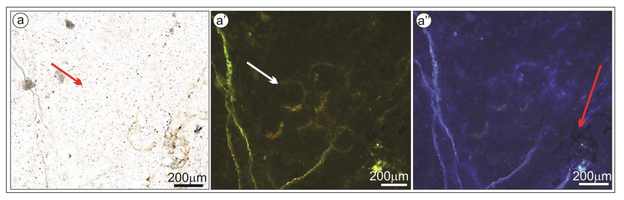

Figure 7: Photomicrographs of early silica preservation of potential microfossils. (a, a', a") Sequence of images showing an aggregate of delicate spheres with an average size of 200µm, with or without – red arrow – enveloped walls (a, PPL) and their distinctive orange fluorescence response of the wall under UV light (a', a"), suggesting a possible organic coating. Dark colored of matured organic films in UV light (red arrow) (a").

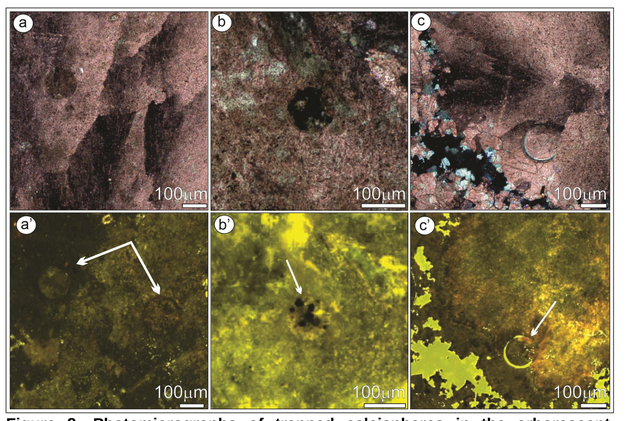

Figure 8: Photomicrographs of trapped calcispheres in the arborescent shrubstones. The calcispheres, with an average size of 100 µm, feature a peloidal micritic (a) or a microcrystalline calcite (c) nuclei, often replaced by pyrite (b, b' – white arrow).They typically are coated by dark-colored micritic wall (a' –white arrow) that is often dissolved displaying a moldic porosity (c').

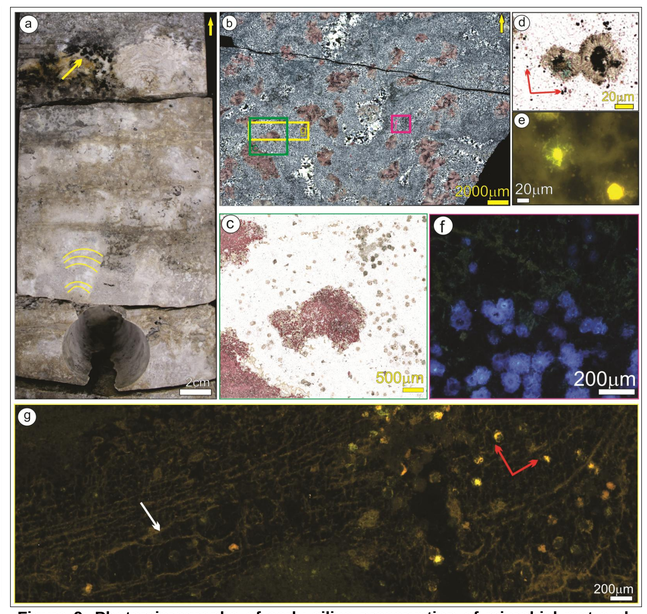

Figure 9: Photomicrographs of early silica preservation of microbial mat and potential microfossils. (a) Completely silicified columnar shrubstone with domal features marking growth (yellow lines), fractures, and abundant hydrocarbon clusters (yellow arrow).(b) Thin section from (a), showing a siliceous matrix composed of microcrystalline quartz, macrocrystalline quartz(voids), and chalcedony spherulites (CS) in XPL; squares indicate the sequence of highlighted images.(c) Detailed view of corroded calcite spherulites embedded in a siliceous matrix rich in CS in PPL. (d) CS with organic-rich and dark nuclei with the black dots (red arrows) resemble microfossils observed by Moore et al. (2024) in the Barra Velha Formation. (e) CS showing bright yellow fluorescence under UV light (long wave). (f) CS showing bright blue fluorescence under UV light (short wave). (g) Microbial mats showing light yellow fluorescence under UV light (long wave), with a reticulated pattern indicating horizontal (white arrow) and vertical growth of mats; CS display bright yellow responses (red arrows).

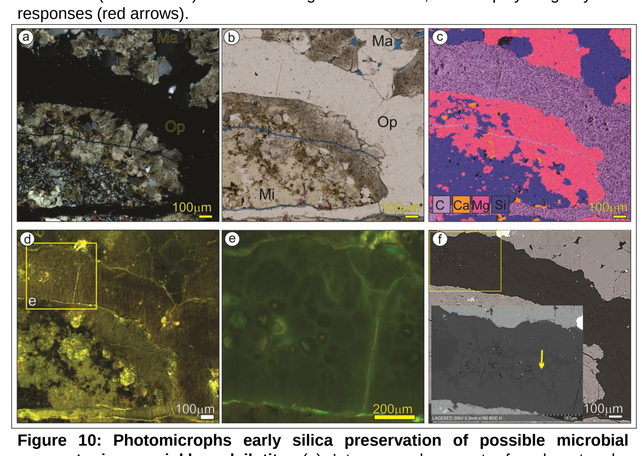

Figure 10: Photomicrophs early silica preservation of possible microbial remnants in a wrinkly calcilutite. (a) Intense replacement of carbonates by microcrystalline silica (Mi), macrocrystalline silica (Ma), and isotropic opal (Op), with the opal showing no organization or pattern under XPL, and (b) in PPL. (c) Chemical map of the same sample, showing the distribution and enrichment of carbon (C), calcium (Ca), magnesium (Mg), and silica (Si). (d) Bright fluorescence of dolomite and opal and slight fluorescence responses of microcrystalline and macrocrystalline silica under UV light. (e) Detail of (d), showing ghosts of spheres ranging from 20-90µm, resembling clusters of clots entrapped within the opal nodule. (f) SEM image of the potential organic remnants in wrinkly calcilutites/laminites, with the highlighted square showing two holes generated by the spot on a carbon-rich layer.

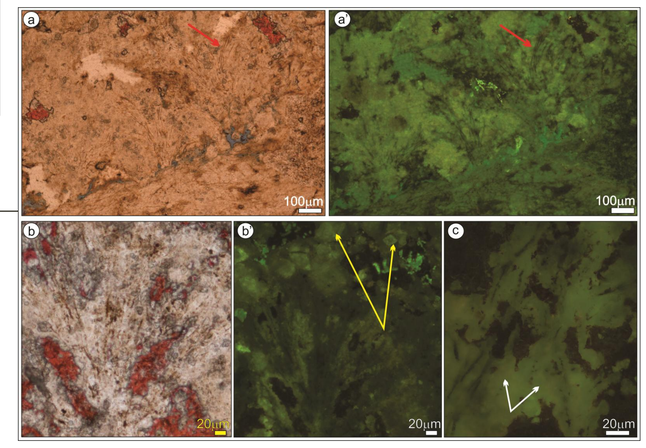

Figure 11: Photomicrographs of early silica preservation of potential microfossils and filaments in Shrubstones and Shrubby Spherulestone. (a) Delicate thin filaments indicated by red arrows in PPL. (a') Corresponding ultraviolet (UV-long wave) fluorescence image, with no fluorescence response. (b) Detailed photomicrograph in plane-polarized light (PPL) providing a close-up view of the replacement of shrubs and their associated filaments. (b') Corresponding UV-fluorescence image of the view in (b), revealing black and gray responses of the calcite and filaments and green responses for the dolomites (yellow arrow). (c) High-magnification close-up under UV light, focusing on the filaments and their immediate surroundings. The image shows slight orange fluorescent material (white arrow), likely from the matrix, that appears to be entrapped within or engulfing the filaments.

Conclusion

Organic remnants and microbial activity are not restricted to the Lula Fingers at Iracema Field. Petrographic microscopy analyses at both macro- and microscales were insufficient to identify filaments, microbial mats, biofilms, and organic remains, even though core analysis showed suggestive features like tepees, domal structures, and crenulated laminations. CL imaging effectively revealed multiple generations of late-stage calcite cements with dark brown to bright red concentric zoning; however, as this technique is not suited for identifying organic matter, it did not highlight remnants. In contrast, fluorescence microscopy proved to be the most effective method, clearly identifying primary features such as filaments, biofilms, and microbial mats. Furthermore, fluorescence highlighted diagenetic characteristics such as engulfed and ghost minerals, organic nuclei, and porosity relationships, even in intensely dolomitized or recrystallized limestones. SEM analyses demonstrated that the organic tissues were replaced by extremely early silica, a common mechanism for preserving such remnants. The high thermal maturation of the Iracema Area is likely a key factor affecting the luminescence response of any remaining organic material.

References

Acknowledgements

This research was carried out in association with the R&D project registered as ANP 23009-4 (PRESAL-II – Impact of tectono-stratigraphic controls on Pre-salt reservoir quality and distribution), funded by Shell Brasil as part of the "Compromisso com Investimentos em Pesquisa e Desenvolvimento" of ANP – Brazilian National Agency of Petroleum, Natural Gas and Biofuels.